Response of an Integrated Building and Free-Field Surface and Downhole Network

by

M. Çelebi[1]

ABSTRACT

An integrated seismic monitoring system with a total of 55 channels of accelerometers is now operating at and in the nearby free-field site of the 20-story steel-framed Atwood Building, in highly seismic Anchorage, Alaska. The building has a single-story basement and a reinforced-concrete foundation without piles. The monitoring system comprises a 32-channel structural and a 21-channel site array. Accelerometers are deployed on 10 levels of the building to assess translational, torsional, and rocking and interstory drift (displacement) between selected pairs of adjacent and average drift between floors. The site array, located approximately a city block from the building, and comprising seven tri-axial accelerometers, one at the surface and six in boreholes ranging in depths from 15 to 200 feet (5-60 meters). The arrays have already recorded responses of the building and the site caused by numerous earthquakes both at distances ranging from tens to a couple of hundred kilometers. Analyses of the responses clearly indicate propagation of seismic waves from the lowest borehole all the way to the roof of the building. Although the response data collected to date are of low-amplitude, they reveal the complete seismic behavior and dynamic characteristics of the building and the site. Data from an earthquake that occurred 186 km away are used to identify the fundamental structural frequency as 0.58 HZ (NS) and 0.47 Hz (EW) and the fundamental site frequency as 1.5 Hz. During the low-amplitude responses recorded from this event, waves propagate in approximately 0.5 seconds from the boreholes to the roof. Mode-coupling and beating effects are identified. Soil-structure interaction effects are not observed at the low levels of recorded motion. The integrated array serves as an example for future instrumentation projects to assess their behavior and performances.

KEYWORDS: real-time monitoring, cable-stayed bridge, New Madrid Seismic Zone, seismic event, acceleration, accelerometer, downhole, internet communication, data acquisition.

1. INTRODUCTION

The Atwood Building is 20 stories tall and is located in highly seismic Anchorage, Alaska (Figure 1). The building is a steel moment-resisting framed (MRF) structure with only one level of basement, 130’x130’ (39.6 m x 39.6 m) in plan with a 48’x48’ (14.6 m x 14.6 m) in-plan center steel-shear walled core, and 264’ (80.5 m) tall. The building foundation is without any piles and consists of a 5’ (1.52 m) thick reinforced concrete mat below the core and a 4’6” (1.37 m) thick reinforced concrete perimeter mat interconnected with grade beams.

The site of the building in downtown Anchorage is underlain by an approximately 100-150-feet (30.5 – 45.7 m) thick soil layer known as the Bootlegger Cove Formation, where considerable ground failures occurred during the 1964 Great Alaska earthquake (Updike and Carpenter, 1986). Built within this geotechnical and seismic environment, Atwood Building, without piles supporting its foundation (exterior and core mats, interconnecting grade beams) and a structural system (MRF steel frame with steel core shear wall) was selected for seismic monitoring. Thus, during earthquakes of various levels of shaking, recording the response and then assessing the behavior of this building and its site can enhance seismic assessment of the behavior and performances of similar buildings during future large earthquakes.

[1] Earthquake Hazards Team, USGS (MS977), 345 Middlefield Rd., Menlo Park, Ca, 94025

The seismic monitoring system of the building comprises and integrates a structural (superstructure and foundation) and a site (surface and downhole) array. The superstructure and foundation array, designed by the author, consists of accelerometers deployed on the basement, at street level, and on the 2^{nd}, 7^{th}, 8^{th}, 13^{th}, 14^{th}, 19^{th} floors (Çelebi, 2003). This configuration, depicted in Figure 1, is designed to detect motion of the building in the E-W and N-S directions, and, in the basement, additionally, in the vertical direction to capture (a) translational, (b) torsional, (c) interstory drift (displacement between selected two consecutive floors) or average drift between any two floors, and (d) rocking of the building.

The structural array is complemented by an extensive freefield site array, located approximately one city block from the building, and consisting of seven tri-axial accelerometers, one at the surface and six in boreholes with depths ranging from 15 to 200 feet [~5-60m] (Figure 1). Removed from the vibrational effects of the building, the associated site array is designed to capture the response of varying layers of soil, and how such layering alters the characteristics of earthquake motions as they travel to the surface and shake the structure. Thus, with the integrated site and superstructure arrays, propagation of motions starting from the lowest downhole depth to the ground surface, basement and the roof of the building are recorded to facilitate structural, site response and soil-structure interaction (SSI) studies. Capturing the propagation and travel time is important as large and abrupt changes may indicate damage to structural members, components and the system.

Since the deployment of the arrays in 2003, numerous small and medium sized earthquakes from near and far sources have been recorded (Çelebi, 2006). The low-amplitude shaking of the building caused by these earthquakes did not cause any damage, but provide opportunities to identify response characteristics of the building and the site. Earlier data sets include responses from only the structure array, as the site array was not yet installed. Yang and others (2004) performed studies of only the data from the building array. This paper introduces and analyses recorded data from both structural and site arrays. However, for sake of brevity, only one set of earthquake response data is included herein.

2. ANALYSES OF STRUCTURAL AND SITE ARRAY DATA : EARTHQUAKE OF APRIL 6, 2005

Acousally-filtered accelerations and computed (double-integrated accelerations) displacements from both the site and the superstructure arrays of the Atwood Building during the April 6, 2005 Tazlina Glacier (AK) earthquake (M_L=4.9), epicenter at 183 Km from the building, are provided in Figure 2 and 3. The largest peak acceleration recorded in the building array is on the order of 0.5% g. The figures clearly show the propagation of waves from basement to the roof of the building. The height of this building is 264 ft [~81m] from ground floor and 275 ft [~85m] from basement. The travel time of waves from the basement to the roof is about 0.5 seconds and, as expected during this low-amplitude shaking event, the propagation of the waves does not indicate abrupt changes (e.g. transients or spikes) to indicate damage to structural members, components and the overall structural system.

Figure 4 shows the roof accelerations and corresponding amplitude spectra of the two parallel NS components, their difference, and the EW component. In the spectra, significant structural frequencies can be identified. Although the torsional response is not significant, the torsional frequencies computed from differential acceleration (CH30-CH31 in the figure) are similar to the predominant frequencies computed from NS and EW motions, indicating possible coupling and also possibly causing the beating effect visually most prominent in the displacement time-history plots (Figure 3).

Figure 5 presents **c**ross-spectrum, coherence and phase angle plots of pairs of NS ([a] CH30 and CH15), EW ([b] CH32 and CH 17) and torsional (differential of NS) accelerations ([c] CH30-CH31 and CH15-CH17) at roof and 8^{th} floor. The pairs of accelerations in each case are perfectly coherent for the modal frequencies indicated, and are 0^o in phase for the lowest frequencies (indication of first mode) and 180^o out of phase for the second and third lowest frequencies (indicating second and higher modes). It is noted again that the frequencies for the torsional responses are similar to the translational frequencies.

Figure 6 shows a sample system identification analysis for the NS building response. Such analyses allows computation of modal damping values in addition to the modal frequencies. The ARX (acronym -- AR for autoregressive and X for extra input) model, based on the least squares method for single input-single output coded in commercially available system identification software (The MathWorks 1988), is used in system identification analyses performed herein (Ljung 1997). Typically the input is the basement or ground floor motion and the output is the roof level motion or one of the levels where the structural response is recorded. The damping ratios are extracted with the procedures outlined by Ghanem and Shinozuka (1995). The figure shows nearly perfect prediction of the roof motions. Results extracted from the analyses are summarized in Table 1 which shows that for the first mode, the modal damping values are relatively low, but this may be due to the low level of shaking. During stronger shaking, expected higher damping will affect the responses. As observed in other studies (Boroschek and Mahin, 1991, Çelebi, 1994), the low level damping and nearly identical translational and torsional frequencies could cause the coupling and beating effect observed in Figure 3 and Figure 6. Repetitively stored potential energy during the coupled translational and torsional deformations turns into repetitive vibrational energy.

Table 1. Dynamic characteristics determined by system identification (ξ=modal damping).

Mode	NS			EW		
	F(Hz)	T(s)	ξ (%)	F(Hz)	T(s)	ξ (%)
1	0.53	1.89	2.7	0.47	2.13	4.2
2	1.83	0.55	2.7	1.53	0.65	2.8
3	3.6	0.28	5.1	2.9	0.35	2.4
4	4.9	0.20	3.6	4.2	0.24	4.1

Figure 7 shows amplitude spectra of (a) NS and (b) EW accelerations in the building (roof, 8th floor and basement) and of (c) and (d) accelerations in the basement and surface and lowest downhole free-field motions. The figure illustrates, at least for the lowest frequencies below 5 Hz, that the building frequencies are different than those of the site. Simple spectral ratios, illustrated in Figure 8, of NS and EW building motions (at the roof and 8th floor with respect to basement) further corroborate and confirm the structural frequencies determined by system identification. The narrow band of the structural frequencies in the amplitude spectra or the spectral ratios reflect the low damping ratios computed by system identification.

Figures 9, 10 and 11 are presented to corroborate site frequencies as determined from records or computation of transfer functions using site borehole data. Figure 9 shows amplitude spectra of NS and EW accelerations and corresponding spectral ratios at basement and the free-field array computed with respect to the lowest borehole at -61m. Significant frequency peaks identified from the figure are approximately 1.2-1.7, 4, 7, and 9.0-9.5 Hz in the NS direction and 1.5, 4.0-4.2, 7 and 9 Hz in the EW direction. It is noted that the fundamental frequency (period) [1.2-1.7 Hz (0.58-0.83 s) NS and 1.5 Hz (0.67 s) EW] at this site are not identical and appear to be azimuthally dependent. These site frequencies are consistent with those of the transfer function computed from the shear wave velocity - depth profile (Cole, pers. comm.., 2003) at site using a software developed by Mueller (pers. comm., 2005) based on Haskell's shear wave propagation method (Haskell, 1953, 1960). In this method, the transfer function is computed using linear propagation of vertically incident SH waves and as input data related to the layered media (number of layers, depth of each layer, corresponding shear wave velocities [V_s], damping, and density), desired depth of computation of transfer function, sampling frequency, half space substratum shear wave velocity and density. Damping (ξ) in the software is provided as Q, a term used by geophysicists, and is related to damping by $\xi = 1/(2Q)$. Q values used in calculating the transfer functions are between 25-60 for shear wave velocities between 200-600 m/s – having been approximately interpolated to vary linearly within these bounds. The resulting transfer function shows significant frequency bands (Figure 10). Furthermore, in Figure 11, the computed transfer function is compared to the spectral ratio obtained from amplitude spectra of NS and EW accelerations at the surface with respect to downhole at 61 m depth. It can be concluded from this figure that the computed and observed transfer function are in reasonably good agreement. The often used simple formula, $T_s=4H/V_s$, requires minimal but reasonable characterization of depth to bedrock and representative average shear wave velocities of layered media (International Building Code, 2000). Computing average Vs = 300-350 m/s using the formula $V_s(ave)=H/(\Sigma (h_i/V_{si})$, and a depth H=50 m., T_s =0.57-0.67 (or f_s=1.5-1.75 Hz), similar to the computed and observed site period.

Soil-structure interaction (SSI) effects were found not to be significant during the low-amplitude shaking caused by this distant small earthquake. Even though the vertical motions at the basement are not identical for the three locations, no phase differences were observed. As a result, no rocking effects have been identified. Stronger shaking at the site and building from future earthquake may reveal such effects.

3. CONCLUSIONS

An integrated structural and site response monitoring array at the Atwood Building in downtown Anchorage, AK has recorded numerous small to medium earthquakes that occurred at near and far distances. It is expected that in the future, during stronger shaking, important data sets will be obtained. Analysis of the data from an earthquake that occurred at 186 km distance facilitates computation of significant structural frequencies [e.g. fundamental mode NS 0.58 Hz and EW 0.47 Hz]. Low damping percentages (2-4 %) are identified. Torsional motions are closely coupled with translational motions as they exhibit similar frequencies and cause beating effects. No SSI effects are observed. The Fundamental site frequency is identified to be around 1.5 Hz from the records and also from the transfer function computed with actual borehole data.

4. REFERENCES

Boroschek, R. L., and Mahin, S. A., 1991, Investigation of the seismic response of a lightly-damped torsionally-coupled building: Univ. of California, Berkeley, Earthquake Engineering Research Center Report UCB/EERC-91/18, 291pp

Çelebi, M., 2003. Seismic Instrumentation Plan for Robert B. Atwood Building, Anchorage, AK 99501., Administrative Report, United States Geological Survey.

Çelebi, M., 2005, Recorded Earthquake Responses from the Integrated Seismic Monitoring Network of the Atwood Building, Anchorage, (AK), (*in print*) Earthquake Spectra.

Çelebi, M., 2004.Responses of a 14-Story (Anchorage, Alaska) Building to Far-Distance (M_w=7.9) Denali Fault (2002) and Near Distance Earthquakes in 2002, Earthquake Spectra, Journal of EERI, *Earthquake Spectra*, vol.20, no.3, pp. 693-706, August 2004.

Ghanem, R., and Shinozuka, M., 1995,Structural System Identification. I: Theory, ASCE Journal of Engineering Mechanics, v.121, no. 2, pp. 255-264, February 1995.

Haskell, N. A., 1953. The dispersion of surface waves on multi-layered media. *Bull. Seis. Soc. Am.*, 43(1), 17-34.

Haskell, N. A., 1960, Crustal reflection of plane SH waves, *J.Geophysical Res.,*65(12), 4147-4150.

Ljung, L., 1997. System Identification – Theory for the User, Prentice-Hall, 519 p.

The MathWorks, 1998 (and 1995 editions). User Guide: System Identification Toolbox for the User with Matlab, The MathWorks Inc., South Natick, Mass., 200p.

Updike, R. G., and Carpenter, B. A., 1986. Engineering Geology of the Government Hill Area, Anchorage, Alaska. U.S. Geological Survey Bulletin No. 1588. 36p.

Yang. Z., Dutpa, U., Çelebi, M., Liu, H., Biswas, N., Kono, T, and Benz, H., 2004. Strong Motion
Instrumentation and Structural Response of Awood Building in Downtown Anchorage, Alaska, PROC. 13WCEE, Vancouver, B.C., Canada.(CD-ROM).

ACKNOWLEDGEMENTS

Thanks to J. Steidl and U. Dutta for making some of the borehole data available. USGS-NSMP Data Center, managed by C. Stephens, diligently process, store and disseminate the data.

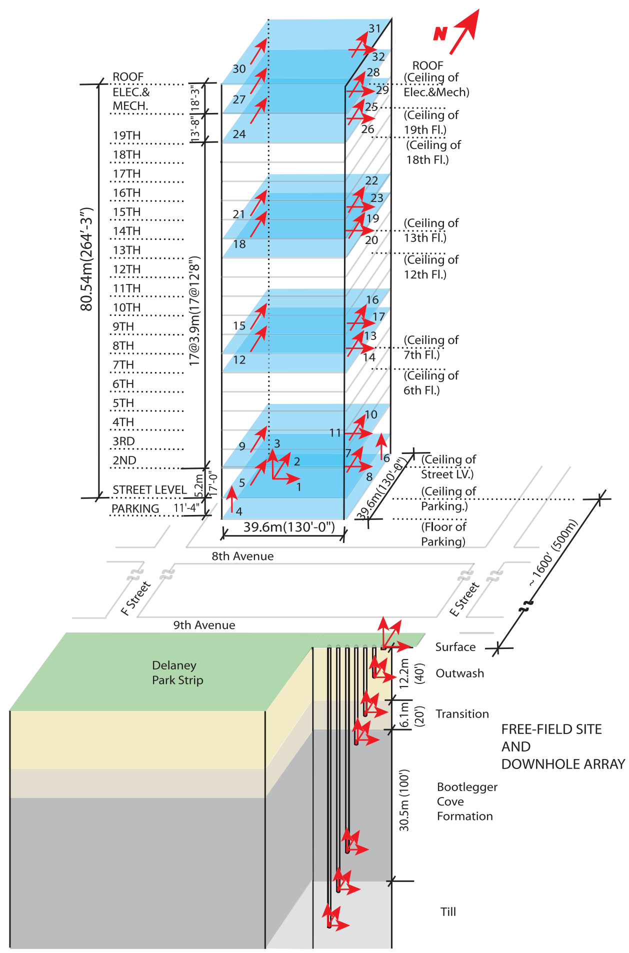

Figure 1. Three-dimensional schematic of the Atwood Building (Anchorage, AK) showing the general dimensions and locations of accelerometers deployed within the structure and at free field with tri-axial downhole accelerometers. The sub-arrays (e.g. superstructure, foundation, surface and downhole free-field sub-arrays) of this particular building monitoring scheme are designed to capture (rocking) SSI effects in addition to the traditional translational and torsional responses.

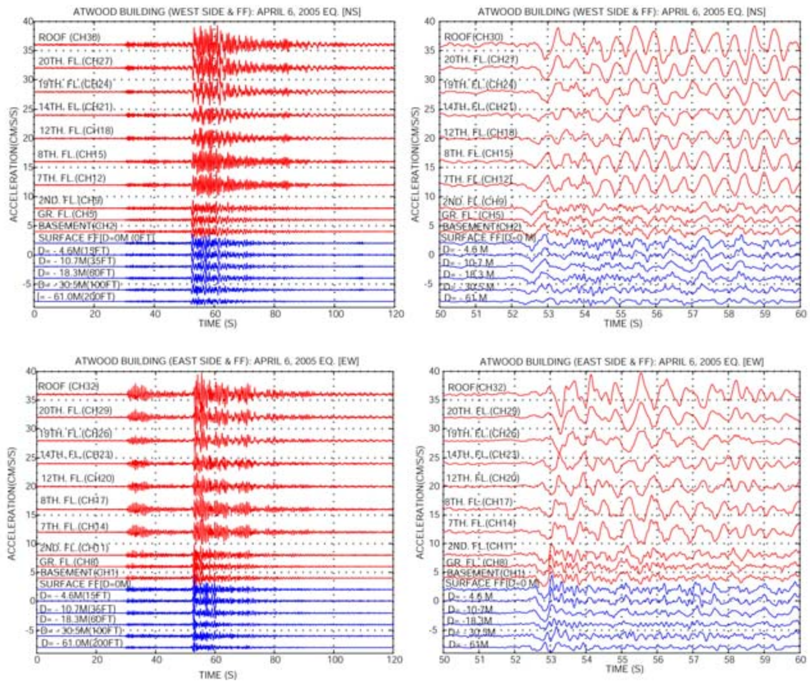

Figure 2. NS (upper panels) and EW (lower panels) accelerations from both the structure and site arrays. The 10-second records on the right are expanded views between 50-60 seconds of the longer records on the left, and show in detail the propagation of S-wave from the lowest downhole depth to the roof of the building. (Note: vertical axes are not in scale with the vertical elevations)**.**

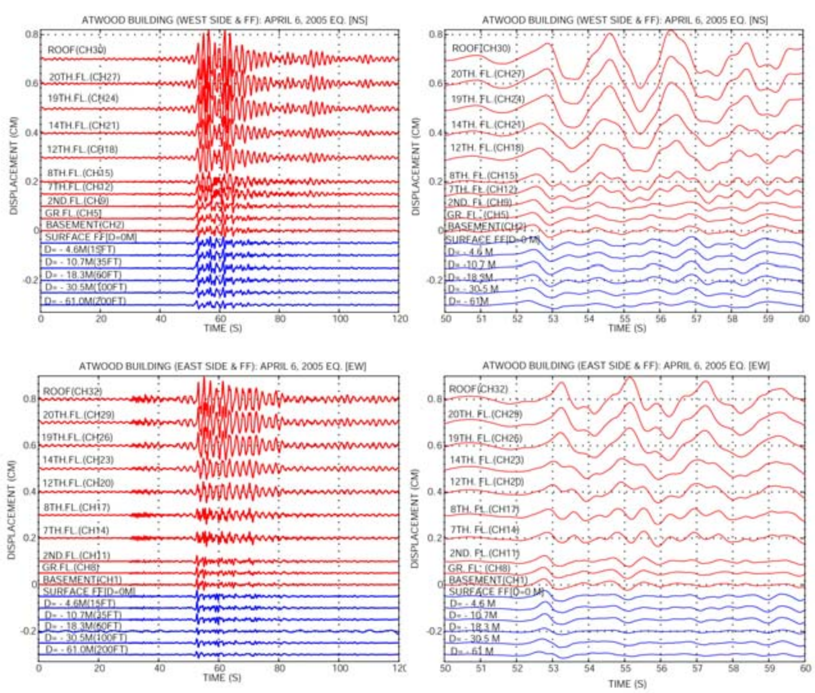

Figure 3. NS and EW displacements corresponding to Figure 2. (Note: vertical axes are not in scale with the vertical elevations).

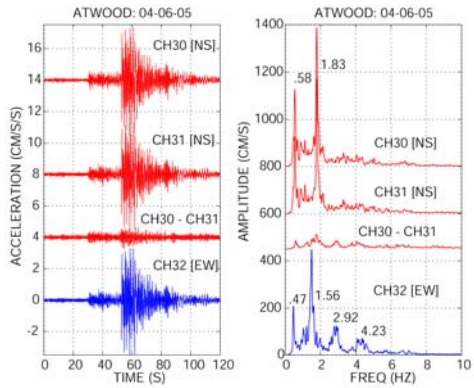

Figure 4. Roof acceleration time-histories and corresponding amplitude spectra.

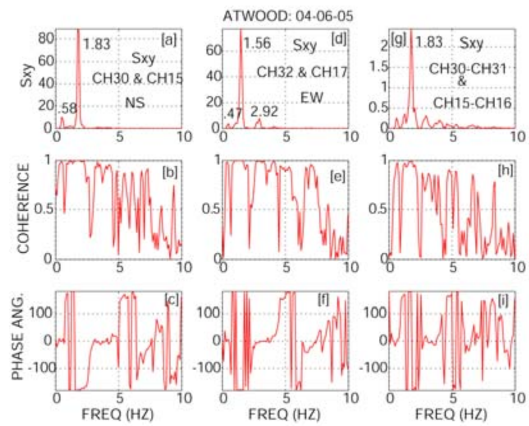

Figure 5. Cross-spectrum, coherence and phase angle plots of pairs of NS (CH30 and 15), EW (CH32 and CH 17) and differential of NS accelerations (CH30-CH31 and CH15-CH17) at roof and 8th floor identifies significant frequencies and associated modes.

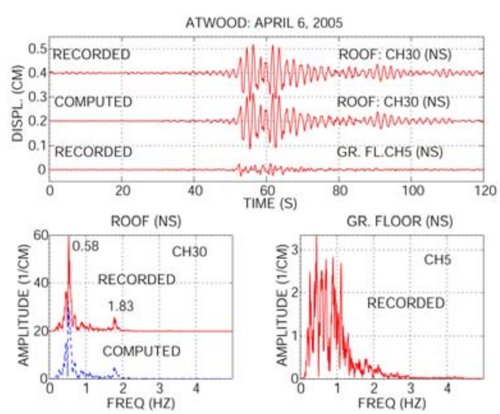

Figure 6. System identification of NS displacements (CH 5 at the ground floor is used as input and Ch 30 as the output). The recorded and computed roof displacements and their amplitude spectra are nearly perfectly matched.

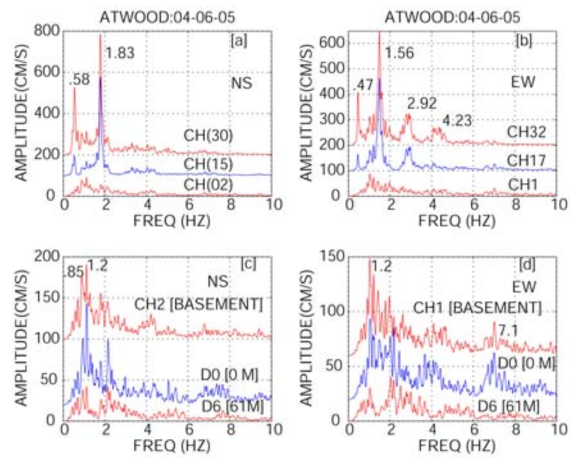

Figure 7. Amplitude spectra of (a) NS and (b) EW accelerations in the building (roof [CH30], 8th floor [CH15] and basement [CH2]) and of (c) and (d) accelerations in the basement and surface [D0] and lowest downhole [D6] free-field motions.

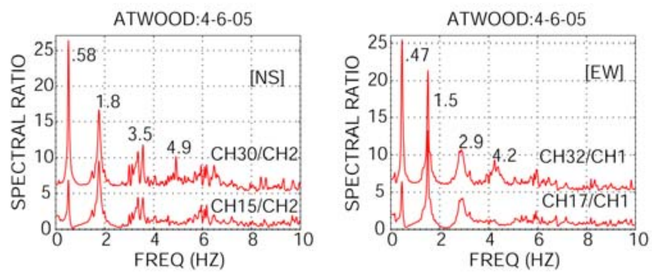

Figure 8. Spectral ratios computed from amplitude spectra of NS and EW accelerations at the roof and 8th floor with respect to those at basement.

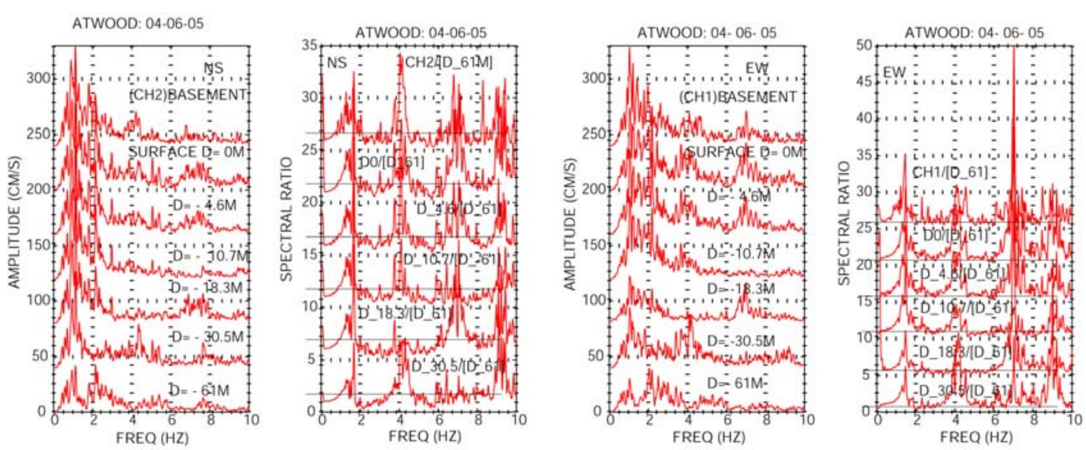

Figure 9. Amplitude spectra and corresponding spectral ratios computed from the amplitude spectra of NS and EW acceleration at basement and the free-field array computed with respect to the lowest borehole at -61m.

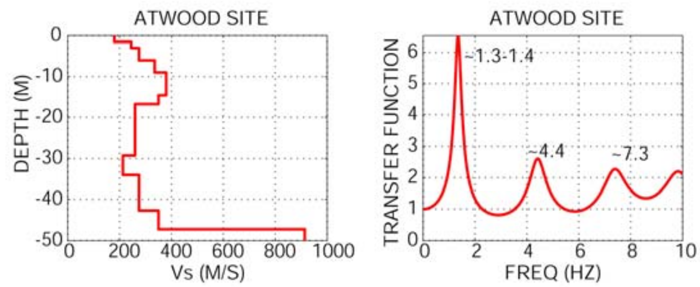

Figure 10. Shear wave velocity (V_s) - depth profile and the computed transfer function.

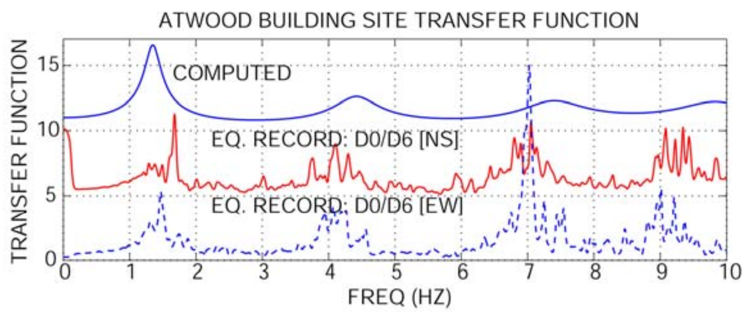

Figure 11. Comparison of computed transfer function to the spectral ratio of amplitude spectra of NS and EW accelerations at the surface with respect to downhole at 61 m depth.